Shang, L., Williams-Jones, A.E., Wang, X., Timofeev, A., Hu, R., Bi, X., 2020.
An Experimental Study of the Solubility and Speciation of MoO3(s) in Hydrothermal Fluids at Temperatures up to 350°C.
Economic Geology, 115(3): 661-669.

An experimental study of the solubility and speciation of MoO_3(s) in hydrothermal fluids at temperatures up to 350 °C

Linbo Shang[a,b*], A.E. Williams-Jones[b], Xinsong Wang[a,b], A. Timofeev[b], Ruizhong Hu[a], Xianwu Bi[a]

[a] *State Key Laboratory of Ore Deposit Geochemistry, Institute of Geochemistry, Chinese Academy of Sciences, Guiyang 550081, China*

[b] *Department of Earth & Planetary Sciences, McGill University, 3450 University Street, Montreal, QC H3A 0E8, Canada*

E-mail address: shanglinbo@vip.gyig.ac.cn (Linbo Shang)

Keywords: molybdenum; solubility; aqueous speciation; hydrothermal fluids; ore formation

Abstract

The solubility of molybdenum trioxide (MoO_3(s)) in aqueous solutions has been investigated experimentally at 250, 300 and 350 °C and saturated water vapor pressure, and total Na concentrations ranging from 0 to 3 m. Results of these experiments show that the solubility of MoO_3(s) increases with increasing temperature and at 350 °C can reach several thousand ppm at high salinity (> 1 m NaCl). At low Na^+ activity, MoO_3(s) dissolves dominantly as $HMoO_4^-$, whereas at high Na^+ activity, the dominant species is $NaHMoO_4^0$. The two dissolution reactions are:

$$MoO_3(s) + H_2O = HMoO_4^- + H^+ \quad (1)$$

$$MoO_3(s) + H_2O + Na^+ = NaHMoO_4^0 + H^+ \quad (2)$$

The values of the logarithms of the equilibrium constants for Reaction 1 are -5.20 ± 0.12，-5.31 ± 0.17 and -5.50 ± 0.09 at 250, 300 and 350 °C respectively, and for Reaction 2 are -3.40 ± 0.11, -3.25 ± 0.19 and -2.97 ± 0.09 for the same temperatures. In combination, these equilibrium constants yield equilibrium constants for the reaction relating the two aqueous species,

$$Na^+ + HMoO_4^- = NaHMoO_4^0 \quad (3)$$

The values of the logarithms of the equilibrium constants for Reaction 3 are 1.80 ± 0.16, 2.06 ± 0.25 and 2.53 ± 0.13 at 250, 300 and 350 °C, respectively. Calculations, based on the results of this study and thermodynamic data available for other species, suggest

strongly that in ore-forming hydrothermal systems, molybdenum is transported mainly as $NaHMoO_4^0$ and deposits as molybdenite in response to cooling and possibly a reduction in fO_2.

Introduction

Molybdenum is a rare element with a very low abundance of 1.1 ppm in the upper continental crust and an even lower abundance in the mantle (50 ppb) (McDonough and Sun, 1995; Rudnick and Gao, 2003). Despite this, molybdenum may be concentrated by hydrothermal fluids to levels in excess of 0.1 wt.% Mo (Ulrich and Mavrogenes, 2008; Zhang et al., 2012; Audétat and Li., 2017), which is sufficient for economic exploitation. Indeed, the global resources of molybdenum are entirely the products of such concentration, mostly in the form of porphyry Mo and Cu-Mo deposits that develop from hydrothermal fluids exsolved from felsic magmas (Mutschler et al., 1999; Zeng et al., 2013; Zhang et al., 2014; Audétat and Li., 2017).

Previous studies investigating the solubility and speciation of molybdenum in hydrothermal fluids have generally concluded that the Mo is transported mainly in the 6+ state as molybdic acid (H_2MoO_4) and its dissociation products $HMoO_4^-$ and MoO_4^{2-} (Candela and Holland,1984; Wood et al., 1987; Keppler and Wyllie, 1991; Minubayeva and Seward, 2010). Among these species, $HMoO_4^-$ is predicted to dominate Mo transport, except at low temperature, for which $H_2MoO_4^0$ and MoO_4^{2-} also play a role at acidic and near-neutral to alkaline conditions, respectively (Ivanova, 1975; Kudrin, 1985; Wood et al.,1987; Minubayeva and Seward, 2010; Dadze et al., 2014, 2017a; Williams-Jones and Migdisov, 2014). The high salinity (> 1 m NaCl) of the fluids interpreted to be responsible for the formation of porphyry Mo and Cu-Mo deposits (Audétat and Li., 2017), however, suggests that species involving Na and/or Cl may also play a role in molybdenum transport. Recognizing this possibility, a number of studies have investigated the effect of salinity (NaCl) on molybdenum solubility (e.g., Kudrin, 1989; Cao 1989; Ulrich and Mavrogenes, 2008; Bali et al., 2012; Zhang et al., 2012, Tattitch and Blundy 2017; Dadze et al., 2018). Although these studies have

proposed species involving Na, e.g., $NaHMoO_4^0$ (Kudrin, 1989; Cao,1989), or Cl, e.g., $MoO_mCl_n^{6-2m-n}$ (Ulrich and Mavrogenes, 2008; Borg et al., 2012), to our knowledge, only Kudrin (1989) and Cao (1989) have reported equilibrium constants for reactions involving these species.

In view of the limited data available on the speciation of Mo in NaCl-bearing fluids and their potential importance in the genesis of hydrothermal Mo deposits, we conducted a series of experiments in order to quantitatively evaluate this speciation Here, we report the results of experiments designed to determine the solubility of molybdenum trioxide in aqueous fluids as a function of salinity and pH at temperatures up to 350 °C. The data are used to evaluate the aqueous speciation of molybdenum at the different conditions and determine the equilibrium constants for reactions involving the dominant species. Using these constants, we then address the question of whether species other than molybdic acid and its dissociation products could play a significant role in the transport of molybdenum in ore-forming hydrothermal systems.

Methods

The solubility of MoO_3(s) in NaCl-bearing aqueous solutions was investigated experimentally at 250, 300 and 350 °C and vapor-saturated water pressure. This involved dissolving MoO_3(s) obtained from Alfa Aesar (99.999% pure) in a series of batch solutions with variable pH and salinity that were prepared for the purpose. The solubility of MoO_3(s) in these solutions and its dependence on salinity and pH were then determined and used to evaluate the solubility product of MoO_3(s) and the stability constants of reactions involving the dominant molybdenum species. As experiments involving NaCl do not allow us to readily separate the effects of complexes involving Na from those involving Cl, we also evaluated the solubility of MoO_3(s) in sodium-triflate ($NaCF_3SO_3$) aqueous solutions. As the triflate ion is non-complexing, i.e., interactions between this ion and metals like Mo^{6+} are extremely weak (Fabes and Swaddle, 1975; Palmer and Drummond, 1988; Applegarth et al., 2015), any increase in Mo concentration with increasing concentration of sodium triflate can be attributed to

ion-pairing of $HMoO_4^-$ or MoO_4^{2-} with Na^+. However, although the triflate ion is stable to temperatures > 400 °C in solutions with near neutral pH, it begins to decompose at temperatures above 280 °C in highly acidic solutions (Applegarth et al., 2015). Our experiments with sodium-triflate solutions were therefore limited to the 250 °C isotherm.

The experimental method used in this study is similar to that of previous studies in our laboratory (e.g., Migdisov and Williams-Jones, 2005; Timofeev et al., 2018), Prior to the experiments, the solid (MoO_3(s)) was introduced into a short silica-glass holder capped with quartz wool to serve as a barrier preventing the solid from entering the autocalves directly but permitting interaction between the solid and the solution during the experiments. In order to ensure that oxygen fugacity remained high enough to preclude formation of Mo(IV) species, a second silica glass, quartz wool-capped holder containing the oxygen buffer Mn_2O_3(s)/Mn_3O_4(s) was prepared; the oxygen fugacity in equilibrium with this buffer greatly exceeds the oxygen fugacity of the MoO_3(s)/MoO_2(s) transition (Robie and Hemingway, 1995). The two holders and 15 - 20 ml of the experimental solution were placed in a titanium autoclave (grade 2 ASTM B348). The holders were designed such that during the experiments, the top of the holder containing the buffer was well above the vapor/liquid interface, whereas the holder containing the MoO_3(s) was immersed in liquid (Fig. 1).

The autoclaves were heated in a Fisher Forced draft oven inside an aluminum box with 1.5 cm thick walls to minimize temperature gradients. The thermal gradient in this system was determined to be < 1 ºC for the entire height of the oven (45cm) by Migdisov and Williams-Jones (2007). The duration of experiments was 7 - 10 days, which has been shown to be sufficient to ensure a steady-state solubility for experiments involving Mo (Rempel et al., 2006, Hurtig and Williams-Jones, 2014). After each experiment, the autoclaves were quenched to room temperature in cold water and opened, and the holders containing MoO_3(s) and the oxygen buffer were removed. A 2 ml aliquot of solution was withdrawn from each autoclave and used to determine the pH. This was followed by the addition to each autoclave of a 3 ml aliquot of a solution containing equal proportions of nitric acid, hydrochloric acid and nano-pure water to dissolve any

Mo-bearing precipitates that might have formed on the walls of the autoclaves during quenching. The resulting solutions were removed from the autoclaves after 30 minutes, diluted and then analyzed for their molybdenum concentration using Inductively Coupled Plasma Mass Spectrometry (ICP-MS). After the experiments, the MoO_3 solid and buffer were analyzed by X-ray diffraction to confirm that other solids had not formed during the experiments. No additional solids were detected, indicating that the solubility measured in this study corresponded only to the dissolution of MoO_3(s) and that the buffer had behaved as expected.

The pH at the temperature of the experiments (pH_T) was extrapolated from the pH measured in the experimental solutions after quenching (pH_{25^oC}). This was done using the modified extended Debye-Hückel equation for NaCl-dominated solutions (Helgeson et al., 1981; Oelkers and Helgeson., 1990; Oelkers and Helgeson, 1991):

$$\log \gamma_n = -\frac{A \cdot [z_i]^2 \cdot \sqrt{I}}{1 + B \cdot å \cdot \sqrt{I}} + b_\gamma \cdot I + \Gamma \qquad (4)$$

in which A and B are the Debye-Hückel solvent parameters, $å$ the distance of closest approach of an ion i, which is specific to the ion of interest, z the charge of the ion, b_γ the extended parameter for NaCl, Γ a molarity to molality conversion factor, and I the true ionic strength after consideration of all dissolved species.

Results

Identification of dissolved molybdenum species

The results of the experiments at 250, 300 and 350 °C are reported in Table 1. In order to evaluate the relationship between the pH, NaCl concentration and molybdenum solubility, and the stoichiometry of the dominant Mo species, the logarithms of the concentrations of Mo measured in the experimental solutions were plotted as a function of the logarithms of the NaCl concentration (Fig. 2a–c) and pH_T (Fig. 3). From Figure 2, it is evident that for NaCl concentrations ≥ 0.01m, the concentration of Mo increases linearly (~1:1 slope) with the concentration of NaCl for each of the isotherms; for experiments conducted at 300 and 350 °C, the concentration of Mo in the NaCl-free solutions is very similar to that in solutions containing 0.1 m NaCl. The concentration

of Mo in the sodium triflate solutions also increases linearly with sodium triflate molality and does so along the ~1:1 trend produced by the experiments with the NaCl solutions (Fig 2a). This supports the hypothesis that, if the relationship between Mo and NaCl concentration reflects complexation, the resulting species involved Na and not Cl. Finally, we note that the concentration of Mo increases with pH_T in a ratio of log mMo to pH that is close to unity (Fig. 3).

Based on the approximately 1:1 dependence of the logarithm of Mo solubility on the logarithm of NaCl concentration and pH, for NaCl concentrations ≥ 0.1 m NaCl, and its independence from NaCl concentration at lower concentrations of the latter, we interpret the solubility of Mo to have been controlled by the formation of two aqueous molybdate species. One of these species is $HMoO_4^-$, which formed as a result of the reaction:

$$MoO_3(s) + H_2O = HMoO_4^- + H^+ \quad (1)$$

The other species is $NaHMoO_4^0$, which formed through the reaction:

$$MoO_3(s) + H_2O + Na^+ = NaHMoO_4^0 + H^+ \quad (2)$$

Calculation of ion activity and derivation of stability constants

As discussed above, $HMoO_4^-$ and $NaHMoO_4$ were identified as the two dominant Mo species in the experimental solutions. At low salinity, $HMoO_4^-$ was the dominant species, whereas $NaHMoO_4$ was dominant at high salinity. The activity of each of the dissolved species and the equilibrium constants for Reactions (1) and (2) were calculated using the methods described in previous publications by our group (e.g., Nisbet et al., 2018; Timofeev et al., 2018; Wang et al., 2019). The standard Gibbs free energy of the aqueous species $HMoO_4^-$ and $NaHMoO_4$ were determined iteratively for each of the isothermal solubility series of experiments using the program OptimA, which is part of the HCh package (Shvarov, 2010 and 2015). This program determines the Gibbs free energy of species by minimizing the sum of squared deviations of the experimentally determined concentrations of the species from the calculated concentrations using the equilibrium composition of the solution.

We considered the following species in our model, H_2O, H^+, OH^-, Na^+, NaOH, NaCl, Cl^-, HCl, MoO_3(s), $HMoO_4^-$ and $NaHMoO_4$ and determined the standard Gibbs free energy of the two molybdenum species from the molality of Mo, NaCl and HCl for each experiment. The molality of HCl was calculated from the starting NaCl concentration and the pH measured after each experiment, which was extrapolated to the experimental temperature using the modified extended Debye-Hückel equation (see Methods). In order to ensure that the solution was saturated with respect to MoO_3(s), an excess amount of this solid was stipulated during the running of OptimA. Excess amounts of the oxygen buffer assemblage were also stipulated. The Haar-Gallagher-Kell (Kestin et al., 1984) and Marshall and Franck (1981) models were used to determine the thermodynamic properties and dissociation constant of H_2O for the experimental conditions. Thermodynamic data for Cl^- were taken from Johnson et al. (1992), for H+ from Wesolowski et al. (1984), for Na^+ and NaOH from Shock et al. (1997), for NaCl from Sverjensky et al. (1997), for HCl from Tagirov et al. (1997) and for MoO_3(s), Mn_2O_3 (s) and Mn_3O_4 (s) from Robie and Hemingway (1995). The Gibbs free energy of $HMoO_4^-$ and $NaHMoO_4$ for each experimental temperature calculated using these data and the method described above are reported in Table 2 together with Gibbs free energy data for other relevant species. Formation constants for these species from MoO_4^{2-}, which were calculated using the Gibbs free energy data reported in Table 2, are reported in Table 3. The uncertainty for each of the values in these tables is that calculated using the OptimA program.

The formation constants for $HMoO_4^-$ and $NaHMoO_4$ reported in Table 3 were fitted to the Ryzhenko-Bryzgalin (MRB) model (Ryzhenko et al., 1985) modified by Borisov and Shvarov (1992) as described in Shvarov and Bastrakov (1999). This was done using the program OptimC in the HCh package (Shvarov, 2010 and 2015). The MRB model was developed to fit the temperature and pressure dependence of dissociation constants for ion pairs through the following equation:

$$\log \mathrm{K}_{(T,P)} = \frac{T_r}{T} \log \mathrm{K}_{(T_r,P_r)} + B_{(T,P)}\left(A_{zz/a} + \frac{B_{zz/a}}{T}\right) \quad (5)$$

in which K is the dissociation constant of the ion pair, T_r and P_r are the reference

temperature and pressure, and $A_{zz/a}$ and $B_{zz/a}$ are fitting parameters. The term $B_{(T,P)}$ accounts for the properties of water at temperature T and pressure P, and was evaluated using the data of Marshall and Franck (1981). The values for the parameters derived from this model for $HMoO_4^-$ and $NaHMoO_4$ are reported in Table 4 together with formation constants for these species determined by the MRB model.

The MRB model and the fitting parameters derived for $HMoO_4^-$ and $NaHMoO_4$ were then used to calculate equilibrium constants (log K) for Reactions (1) and (2) at each temperature investigated experimentally. These constants are reported in Table 5. Reactions 1 and 2 and the corresponding constants, in turn, were combined to yield equilibrium constants for the reaction relating the two aqueous species:

$$Na^+ + HMoO_4^- = NaHMoO_4 \qquad (3)$$

The equilibrium constants for this reaction are also reported in Table 5. Uncertainties associated with the calculation of the equilibrium constants were estimated from the deviation of the measured constants from those obtained using the Gibbs free energy determined by OptimA and optimized using OptimC.

Discussion

Molybdenum speciation

The results of our experiments show that both $HMoO_4^-$ and $NaHMoO_4$ contribute to the solubility of MoO_3(s) in NaCl-bearing aqueous solutions at elevated temperature. We illustrate this in Figure 4, which shows the log activity of the two species (determined using OptimA) as a function of the log activity of Na at 250, 300 and 350 °C for a pH of 2.1. Also shown is the logarithm of the total Mo activity. From this figure, it is evident that at very low activity of Na^+, the solubility of MoO_3(s) is controlled mainly by $HMoO_4^-$ but that even at a Na^+ activity as low 0.02, $NaHMoO_4$ is the dominant aqueous Mo species; at a Na^+ activity above 0.05 the contribution of $HMoO_4^-$ is negligible. The importance of $NaHMoO_4$ also increases with increasing temperature as illustrated in Figure 5, where it can be seen that the predominance boundary for $NaHMoO_4$ moves to lower activity of Na^+ with increasing temperature.

Thus, at 250 °C, approximately 75% of the Mo is dissolved as $NaHMoO_4$, if the salinity is 0.1m, whereas this proportion increases to > 90% at 350 °C for the same salinity. This behaviour may reflect the fact that the dominant species is neutral, which is consistent with the observation that, with increasing temperature, the dielectric constant of water decreases and its hydrogen bonding network weakens cosiderably, thereby favouring aqueous species of low or no charge (Fernández et al.,1997).

Comparison to previous studies

From the results of our experiments, it is clear that the solubility of MoO_3(s) is higher in NaCl-bearing than in NaCl-free aqueous solutions at elevated temperature. The same conclusion has been reached by most previous experimental studies that have investigated the solubility of MoO_3(s) (and MoO_2(s)) in NaCl-bearing and NaCl-free aqueous solutions (Kudrin, 1989; Cao 1989; Ulrich and Mavrogenes, 2008; Bali et al., 2012 ; Zhang et al., 2012 and Dadze et al., 2018). Opinion, however, is divided over whether the higher solubility of Mo in NaCl-bearing aqueous solutions is due to the formation of Na-bearing Mo species (Kudrin, 1989; Cao 1989; Bali et al., 2012), the formation of Cl-bearing Mo species (Ulrich and Mavrogenes, 2008; Dadze et al., 2018) or is simply an artifact of the increased ionic strength of the solution due to the presence of Na^+ and Cl^- (Dadze et al., 2017b). To our knowledge, only Kudrin (1989) has reported stability constants for reactions involving Mo species other than molybdic acid and its dissociation products at elevated temperature. He reported stability constants for the reactions:

$$MoO_2(s) + 0.5\ O_2 + H_2O + Na^+ = NaHMoO_4 + H^+ \quad (6)$$

$$Na^+ + HMoO_4^- = NaHMoO_4 \quad (7)$$

at temperatures between 300 and 450 °C and 500 bar.

In order to compare the results of our experiments with those of Kudrin (1989), which investigated the solubility of MoO_2(s) rather than MoO_3(s) (this study), we based the comparison on Reaction 3. As the pressure employed in the experiments of Kudrin (1989) was 500 bar, the comparison also required correcting for the fact that our experiments were conducted at saturated vapor pressure. We therefore extrapolated our

stability constants to 500 bar using the MRB model. In Figure 6, we compare the equilibrium constants derived for Reaction 3 in our study with those derived from Kudrin (1989). From this figure, it is evident that the results of our study are in excellent agreement with those of Kudrin (1989) at 300 and 350 ºC.

Application to natural systems

As discussed in the introduction of this paper, most of the World's supply of Mo is from porphyry Mo and porphyry Cu-Mo deposits, in which the molybdenum precipitated from magmatic-hydrothermal fluids (e.g., Westra and Keith.,1981; Seedorff et al., 2005; Klemm et al., 2007, 2008; Audétat and Li., 2017). Therefore, the results of our study would be of most relevance, if they could be applied to porphyry Mo and Cu-Mo ore-forming systems. On the basis of fluid inclusion studies for Climax-type deposits, the fluids exsolved from the magmas are interpreted to have contained between 5 and 15 wt% $NaCl_{equiv.}$ (Audétat and Li., 2017), and to have had a total sulfur content of 0.003 m (Audétat., 2015). The pH is generally interpreted to have been buffered by the mineral assemblage, muscovite-K-feldspar-quartz (Seedorff et al., 2005) and oxygen fugacity to have been between 2 and 3.5 log units above the fayalite-magnetite-quartz buffer (QFM) (Qiu et al., 2013; Audétat., 2015). Ore formation is typically considered to have taken place at temperatures between 500 and 300 °C (Seedorf et al., 2005; Klemm et al., 2008; Audétat, 2015)

In order to test the applicability of the results of this study to porphyry Mo systems, we modelled the solubility of molybdenite in an ore-forming magmatic fluid, which had a salinity ranging from 1 m NaCl (~ 6 wt.% NaCl) to 3 m NaCl (~18 wt.% NaCl), and cooled from 500 to 300 ºC at 1000 bar (this pressure, which could reflect that for a fluid evolving in a deep porphyry, was chosen to avoid phase separation after exsolution from the magma). The sulfur concentration ($\sum S$) was assumed to be 0.003 m (Audétat., 2015), the pH to have been buffered by the mineral assemblage muscovite-K-feldspar-quartz and fO_2 to have corresponded to 2.2 log units above FMQ. These conditions are the same as those that have been estimated for the Climax porphyry Mo ore-forming system (Audétat, 2015).

In Figure 7, we illustrate the solubility of molybdenite in the above fluid as a function of temperature and salinity. At 500 °C, the concentration increases from ~ 30 to 206 ppm as salinity increases from 0 to 3 m, emphasizing the important role that salinity plays in promoting Mo solubility in porphyry systems. For the trapping temperature (480 - 460 ºC) of fluid inclusions coexisting with decrepitated melt inclusions (and therefore representing the magmatic fluid) in the Climax deposit (Audétat, 2015), the Mo concentration in a 2 m NaCl solution (the salinity of the inclusions was ~1.8 m) is between 64 and 18 ppm. This concentration range is remarkably similar to that reported by Audétat. (2015) for the above fluid inclusions (60 - 5 ppm Mo).

Because Mo is in the 4+ state in molybdenite and is thought to be mobilized in the 6+ state (Williams-Jones and Migdisov, 2014), the state considered in our experiments, it follows that molybdenite deposition will be strongly influenced by oxygen fugacity. In Figure 8, we show the solubility of molybdenite as a function of salinity and fO_2 for a fluid at a temperature of 450 °C and a pressure of 1000 bar. The sulfur concentration and the pH buffer were the same as for Figure 7. From Figure 8, it is evident that a decrease in fO_2 from FMQ + 2.5 to FMQ will result in about an order of magnitude decrease in solubility. The predicted concentrations of Mo in a 2 m NaCl solution at this temperature are 2 ppm, 22 ppm and 52 ppm for a fO_2 corresponding to that of FMQ, FMQ + 2.5, and FMQ + 3.5 at 450 ºC.

In summary, the transport of Mo in hydrothermal fluids is strongly dependent on salinity and temperature. As molybdenite is the only Mo ore-mineral, however, it also follows that oxygen fugacity and reduced sulfur activity (not explicitly addressed) will have a strong influence on whether an otherwise fertile fluid will produce an economically exploitable Mo deposit.

Conclusions

The experimental data reported in this study show that molybdenite dissolves dominantly as $NaHMoO_4$, except at exceptionally low salinity for which $HMoO_4^-$ is the dominant species. This has important implications for our understanding of the transport of molybdenum in nature and particularly for models of ore formation in

porphyry systems, which have been based largely on an assumption that the metal is transported as the species $HMoO_4^-$. The overarching conclusion of the study is that molybdenum transport is favored by high salinity, high temperature and high oxygen fugacity, and that, in principle, any geological process leading to a decrease in the values of any of these parameters could lead to molybdenum ore deposition.

ACKNOWLEDGEMENTS

The experimental work presented in this paper was carried out in the Fluid-Rock Interaction Laboratory, Department of Earth and Planetary Sciences, McGill University. Financial support for the study was provided by the National Key Research and Development Program of China (2016YFC0600204); the National Natural Science Foundation of China (41673067); the Open Research Fund of the State Key Laboratory of Ore Deposit Geochemistry of China and a Chinese Government Scholarship to L.B. Shang from the China Scholarship Council. We gratefully acknowledge the help of Anna Katharina Jung in conducting the ICP-MS analyses, Artaches Migdisov in the data treatment and Olga Vasyukova and Jethro Sanz-Robinson in accessing the facilities of the Fluid-Rock Interaction Laboratory. The manuscript benefitted significantly from reviews by Zoltan Zajacz, Brian Tattich and Associate Editor, Adam Simon.

REFERENCES

Applegarth, L., Alcorn, C., Bissonette, K., Noël, J., and Tremaine, P.R., 2015, Non-complexing anions for quantitative speciation studies using Raman spectroscopy in fused silica high pressure optical cells under hydrothermal conditions: Applied Spectroscopy, v. 8, p. 972-983.

Audétat, A., 2015, Compositional evolution and formation conditions of magmas and fluids related to porphyry Mo mineralization at Climax: Colorado: Journal of petrology, v. 56, p. 1519–1546.

Audétat, A., and Li, W.T., 2017, The genesis of Climax-type Porphyry Mo deposits: Insights from fluid inclusions and melt inclusions: Ore geology reviews, v. 88, p. 436-460.

Bali, E., Keppler, H., and Audétat, A., 2012, The mobility of W and Mo in subduction

zone fluids and the Mo–W–Th–U systematics of island arc magmas: Earth and Planetary Science Letters, v. 351–352, p. 195–207.

Borisov, M.V., and Shvarov, Y.V., 1992, Thermodynamics of Geochemical Processes: Moscow, Moscow State University Publishing House, 254p.

Borg, S., Liu, W., Etschmann, B., Tian, Y., and Brugger, J., 2012, An XAS study of molybdenum speciation in hydrothermal chloride solutions from 25–385 ºC and 600 bar: Geochimica et Cosmochimica Acta, v. 92, p. 292-307.

Candela, P.A., and Holland, H.D., 1984, The partitioning of copper and molybdenum between silicate melts and aqueous fluids: Geochimica et Cosmochimica Acta, v. 48, p. 373-380.

Cao, X.Y., 1989, Solubility of molybdenite and the transport of molybdenum in hydrothermal solutions: Ph. D. thesis, Ames, USA, Iowa State University, 115p

Dadze, T.P., Kashirtseva, G.A., Novikov, M.P., and Plyasunov, A.V., 2017a, Solubility of MoO_3 in acid solutions and vapor-liquid distribution of molybdic acid: Fluid Phase Equilibria, v. 440, p. 64-76.

Dadze, T.P., Kashirtseva, G.A., Novikov, M.P., and Plyasunov, A.V., 2017b, Solubility of MoO_3 in $NaClO_4$ solutions at 573K: Journal of Chemical Engineering data, v. 62, p. 3848-3853.

Dadze, T.P., Kashirtseva, G.A., Novikov, M.P., and Plyasunov, A.V., 2018, Solubility of MoO_3 in aqueous acid chloride-bearing solutions at 573K: Journal of Chemical Engineering data, v. 63, p.1827-1832.

Dadze, T.P., Kashirtseva, G.A., Novikov, M.P., Plyasunov, A.V., and Shapovalov, Y.B., 2014, The solubility of MoO3 in aqueous solutions of HClO4 at T=300 °C and P=100 bar by experimental data: Doklady Earth Sciences, v. 456, p. 548-549.

Fabes, L., and Swaddle T.W., 1975, Reagents for high temperature aqueous chemistry: trifluoromethanesulfonic acid and its salts: Canadian Journal of Chemistry, v.53, p.3053–3059.

Fernández, D.P., Goodwin, A.R.H., Lemmon, E.W., Levelt Sengers, J.M.H., and Williams, R.C., 1997, A formulation for the static permittivity of water and steam at temperatures from 238 K to 873 K at pressures up to 1200 MPa, including derivatives and Debye-Hückel coefficients: Journal of Physical and Chemical Reference Data, v. 26, p.1125–1166.

Helgeson, H.C., Kirkham, D.H., and Flowers, G.C., 1981, Theoretical prediction of the thermodynamic behavior of aqueous electrolytes at high pressures and temperatures: IV. Calculation of activity coefficients, osmotic coefficients, and apparent molal and standard and relative partial molal properties to 600 ºC: American Journal of Science, v. 281, p.1249–1516.

Hurtig, N.C., and Williams-Jones, A.E., 2014, An experimental study of the solubility of MoO_3 in aqueous vapour and vapour-like supercritical fluids: Geochimica et

394 Cosmochimica Acta, v. 136, p. 169-193.
395 Ivanova, G., Lavkina, N., Nesterova, L., Zhudikova, A., and Khodakovskiy, I., 1975,
396 Equilibrium in the MoO_3–H_2O system at 25–300 ºC: Geochemistry international,
397 v. 12, p. 163-176.
398 Johnson, J.W., Oelkers, E.H., and Helgeson, H.C., 1992, SUPCRT92: A software
399 package for calculating the standard molal thermodynamic properties of minerals,
400 gases, aqueous species, and reactions from 1 to 5000 bar and 0 to 1000°C:
401 Computational Geosciences, v. 18, p. 899-947.
402 Keppler, H., and Wyllie, P.J. 1991, Partitioning of Cu, Sn, Mo, W, U, and Th between
403 melt and aqueous fluid in the systems haplogranite-H_2O-HCl and haplogranite-
404 H_2O-HF: Contributions to Mineralogy and Petrology, v. 109, p. 139-150.
405 Kestin, J., Sengers, J.V., Kamgar-Parsi, B., and Levelt Sengers, J.M.H. 1984,
406 Thermodynamic properties of fluid H_2O: Journal of Physical and Chemical
407 Reference Data, v. 13, p. 601–609.
408 Klemm, L., Pettke, T., and Heinrich, C.A. 2007, Hydrothermal evolution of the El
409 Teniente deposit, Chile: porphyry Cu–Mo ore deposition from low-salinity
410 magmatic fluids: Economic Geology, v. 102, p. 1021–1045.
411 Klemm, L.M., Pettke, T., and Heinrich, C.A. 2008, Fluid and source magma evolution
412 of the Questa porphyry Mo deposit, New Mexico, USA: Mineralium Deposita, v.
413 43, p. 533–552.
414 Kudrin, A., 1985, The solubility of tugarinovite MoO_2 in aqueous solutions at elevated
415 temperatures: Geochemistry international, v. 22, p. 126-138.
416 Kudrin, A., 1989, Behavior of Mo in aqueous NaCl and KCl solutions at 300–450 ºC:
417 Geochemistry international, v. 26, p. 87-99.
418 Marshall, W.L., and Franck, E.U., 1981, Ion product of water substance, 0–1000 ºC, 1–
419 10,000 bars new International Formulation and its background: Journal of Physical
420 and Chemical Reference Data, v. 10, p. 295–304.
421 McDonough, W.F., and Sun, S.S., 1995, The composition of the Earth: Chemical
422 Geology, v. 120, p. 223-253.
423 Migdisov, A.A., and Williams-Jones, A.E., 2005, An experimental study of cassiterite
424 solubility in HCl-bearing water vapor at temperatures up to 350°C: Implications
425 for tin ore-formation. Chemical Geology, v. 217, p. 29-40.
426 Migdisov, A.A., and Williams-Jones, A.E., 2007, An experimental study of the
427 solubility and speciation of neodymium (III) fluoride in F-bearing aqueous
428 solutions: Geochimica et Cosmochimica Acta, v. 71, p. 3056-3069.
429 Minubayeva, Z., and Seward, T.M., 2010, Molybdic acid ionisation under hydrothermal
430 conditions to 300ºC: Geochimica et Cosmochimica Acta, v. 74, p. 4365-4374.
431 Mutschler, F.E., Ludington, S., and Bookstrom, A.A., 1999, Giant porphyry-related
432 metal camps of the world - a database. U.S. Geological Survey Open-File Report

433 99-556, Online Version 1.0, (http://geopubs.wr.usgs.gov/open-file/of99-556/).
434 Nisbet, H., Migdisov, A.A., Xu, H., Guo, X., Van Hinsberg, V., Williams-Jones, A.E.,
435 Boukhalfa, H., and Roback, R., 2018, An experimental study of the solubility and
436 speciation of thorium in chloride-bearing aqueous solutions at temperatures up to
437 250 °C: Geochimica et Cosmochimica Acta, v. 239, p. 363-373.
438 Oelkers, E.H., and Helgeson, H.C., 1990, Triple-ion anions and polynuclear
439 complexing in supercritical electrolyte solutions: Geochimica et Cosmochimica
440 Acta, v. 54, p. 727–738.
441 Oelkers, E.H., and Helgeson, H.C., 1991. Calculation of activity coefficients and
442 degrees of formation of neutral ion pairs in supercritical electrolyte solutions:
443 Geochimica et Cosmochimica Acta, v. 55, p. 1235-1251.
444 Palmer, D.A., and Drummond, S.E., 1988, The molal dissociation quotients of water in
445 sodium trifluorosulfonate solutions at high temperatures: Journal of Solution
446 Chemistry, v. 17, p. 153-164.
447 Qiu, J.T., Yu, X.Q., Santosh, M., Zhang, D.H., Chen, S.Q., and Li, P.J., 2013,
448 Geochronology and magmatic oxygen fugacity of the Tongcun molybdenum
449 deposit, northwest Zhejiang, SE China: Miner Deposita, v. 48, p. 545-556.
450 Rempel, K.U., Migdisov, A.A., and Williams-Jones, A.E., 2006, The solubility and
451 speciation of molybdenum in water vapour at elevated temperatures and pressures:
452 Implications for ore genesis: Geochimica et Cosmochimica Acta, v. 70, p. 687-696.
453 Robie, R.A., and Hemingway, B.S., 1995, Thermodynamic properties of minerals and
454 related substances at 298.15 K and 1 bar (10^5 pascals) pressure and at higher
455 temperatures: U. S. Geological Survey Bulletin 2131, 461p.
456 Rudnick, R., and Gao, S., 2003, Composition of the continental crust: Treatise on
457 geochemistry, v. 3, p. 1-64.
458 Ryzhenko, B.N., Bryzgalin, O.V., Artamkina, I.Y., Spasennykh, M.Y., and Shapkin, A.
459 I., 1985, An electrostatic model for the electrolytic dissociation of inorganic
460 substances dissolved in water: Geochemistry international, v. 22, p. 138–144.
461 Seedorff, E., Dilles, J.H., Proffett, J.M.J., Einaudi, M.T., Zurcher, L., Stavast, W.J.A.,
462 Johnson, D.A., and Barton, M.C., 2005, Porphyry deposits: characteristics and
463 origin of hypogene features: Economic Geology, 100th anniversary volume, p.
464 251–298.
465 Shock, E.L., Sassani, D.C., Willis, M., and Sverjensky, D.A., 1997, Inorganic species
466 in geologic fluids: Correlations among standard molal thermodynamic properties
467 of aqueous ions and hydroxide complexes: Geochimica et Cosmochimica Acta, v.
468 61, p. 907-950.
469 Shvarov, Y.V., and Bastrakov, E., 1999, HCh, A Software Package for Geochemical
470 Equilibrium Modeling: User's Guide: Record 1999/25.
471 Shvarov, Y.V., 2010, OptimA: A program for the calculation of the free energies of

dissolved aqueous species from the results of chemical experiments. (http://www.geol.msu.ru/deps/geochems/soft/).

Shvarov, Y.V., 2015, A suite of programs, OptimA, OptimB, OptimC, and OptimS compatible with the Unitherm database, for deriving the thermodynamic properties of aqueous species from solubility, potentiometry and spectroscopy measurements: Applied Geochemistry, v. 55, p.17-27.

Sverjensky, D.A., Shock, E.L., and Helgeson, H.C., 1997, Prediction of the thermodynamic properties of aqueous metal complexes to 1000°C and 5 kb: Geochimica et Cosmochimica Acta, v. 61, p.1359-1412.

Tagirov, B.R., Zotov, A., and Akinfiev, N., 1997, Experimental study of dissociation of HCl from 350 to 500 ºC and from 500 to 2500 bars: thermodynamic properties of HCl(aq): Geochimica et Cosmochimica Acta, v. 61, p. 4267–4280.

Tattitch, B. C., and Blundy J. D., 2017, Cu-Mo partitioning between felsic melts and saline-aqueous fluids as a function of XNaCleq, fO_2, and fS_2 : American Mineralogist, v.102, p.1987-2006.

Timofeev, A., Migdisov, A.A., Williams-Jones, A.E., Roback, R., Nelson, A.T., and Xu, H.W., 2018, Uranium transport in acidic brines under reducing conditions: Nature, v. 9, p. 1469.

Ulrich, T., Günther, D., and Heinrich, C.A., 2002, The evolution of a porphyry Cu-Au deposit, based on LA-ICP-MS analysis of fluid inclusions: Bajo de la Alumbrera, Argentina: Economic Geology, v. 97, p. 1889–1920.

Ulrich, T., and Mavrogenes, J., 2008, An experimental study of the solubility of molybdenum in H_2O and KCl–H_2O solutions from 500° C to 800° C, and 150 to 300MPa: Geochimica et Cosmochimica Acta, v. 72, p. 2316-2330.

Wang, X-S., Timofeev, A., Williams-Jones, A.E., Shang, L-B, and Bi, X-W, 2019, An experimental study of the solubility and speciation of tungsten in NaCl-bearing aqueous solutions at 250, 300 and 350 °C: Geochimica et Cosmochimica Acta, v. 265, p. 313-329.

Westra, G., and Keith, S.B., 1981, Classification and genesis of stockwork molybdenum deposits: Economic Geology, v. 76, p. 844–873.

Williams-Jones, A.E., and Migdisov, A.A., 2014, Experimental constraints on the transport and deposition of metals in ore-forming hydrothermal systems: In Kelley K.D., and Golden H.C., eds., Building Exploration Capability for the 21st Century, Society of Economic Geologists Special Publication, No. 18, p. 77-95.

Wood, S.A., Crerar, D.A., and Borcsik, M.P., 1987, Solubility of the assemblage pyrite-pyrrhotite-magnetite-sphalerite-galena-gold-stibnite-bismuthinite-argen-tite-molybdenite in H_2O-NaCl-CO_2 solutions from 200 to 350 ºC: Economic Geology, v. 82, p. 1864-1887.

Zeng, Q.D., Liu, J.M., Qin, K.Z., Fan, H.R., Chu, S.X., Wang, Y.B., and Zhou, L.L.,

2013, Types, characteristics, and time–space distribution of molybdenum deposits in China: International Geology Review, v. 55, p. 1311–1358.

Zhang, H., Li, C.Y., Yang, X.Y., Sun, Y.L., Deng, J.H., Liang, H.Y., Wang, R.L., Wang, B.H., Wang, Y.X., and Sun W.D., 2014, Shapinggou: the largest Climax-type porphyry Mo deposit in China: International Geology Review, v. 56, p. 313-331.

Zhang, L., Audétat, A., and Dolejš, D., 2012, Solubility of molybdenite (MoS_2) in aqueous fluids at 600–800 °C, 200MPa: A synthetic fluid inclusion study: Geochimica et Cosmochimica Acta, v. 77, p. 175-185.

Figure captions

Fig. 1. A sketch of the experimental set-up used in this study.

Fig. 2. The logarithm of Mo molality as a function of the logarithm of NaCl molality at 250, 300 and 350 °C (red dots) and as a function of the logarithm of $NaCF_3SO_3$ (sodium triflate) molality at 250 °C (blue diamonds). The uncertainty for each datum is less than the diameter of the symbol.

Fig. 3. The logarithm of Mo molality as a function of pH_T at 300 (brown) and 350 (green) °C .

Fig. 4. Values of log aΣMo (blue dots), log a$NaHMoO_4$ (red dashed line) and log a$HMoO_4^-$ (green dashed line) as a function of log aNa^+ at 250 (a), 300 (b) and 350 °C (c). The values were obtained from equilibrium constants for Reactions (1) and (2) calculated using OptimA, and are normalised to a pH of 2.1.

Fig. 5. a) Predominance fields of $HMoO_4^-$ and $NaHMoO_4$ as a function of temperature and log aNa^+. b – d) The distribution of Mo (VI) aqueous species as a function of log aNa^+ at 250 °C, 300°C and 350°C, respectively. The diagrams are based on data for the equilibrium constants of Reaction 3.

Fig. 6. Equilibrium constants for Reaction 3 determined in this study (red squares), fitted to the BR model (black dashed line) at Psat, and corrected to 500bar (red dashed line) for comparison to the constants derived from Kudrin (1989) for this pressure (blue dots).

Fig. 7. The concentration of Mo at molybdenite saturation and 1000 bar, as a function of temperature in solutions containing 0 to 3 m NaCl, 0.5 m KCl, and 0.003 m ΣS; pH is buffered by the assemblage, muscovite-K-feldspar-quartz, and fO_2 is fixed at 2.2 log units above the fayalite-magnetite-quartz (FMQ + 2.2) buffer. The calculations were performed using HCh (Shvarov,

2008) and thermodynamic data for aqueous Mo species from this study ($HMoO_4^-$ and $NaHMoO_4$) and Shock, 1997 (H_2MoO_4 and MoO_4^{2-}).

Fig. 8. The concentration of Mo at molybdenite saturation, 450 °C and 1000 bar, as a function of oxygen fugacity in solutions containing 0 to 3 m NaCl, 0.5 m KCl, and 0.003 m ΣS; pH is buffered by the assemblage, muscovite-K-feldspar-quartz. The calculations were performed using HCh (Shvarov, 2008) and thermodynamic data for aqueous Mo species from this study ($HMoO_4^-$ and $NaHMoO_4$) and Shock, 1997 (H_2MoO_4 and MoO_4^{2-}).

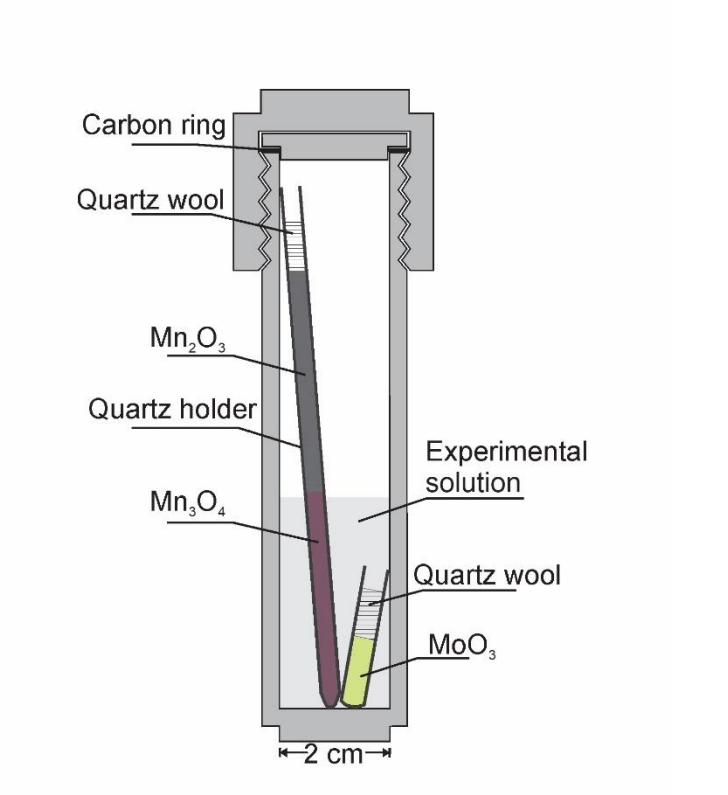

Fig. 1. A sketch of the experimental set-up used in this study.

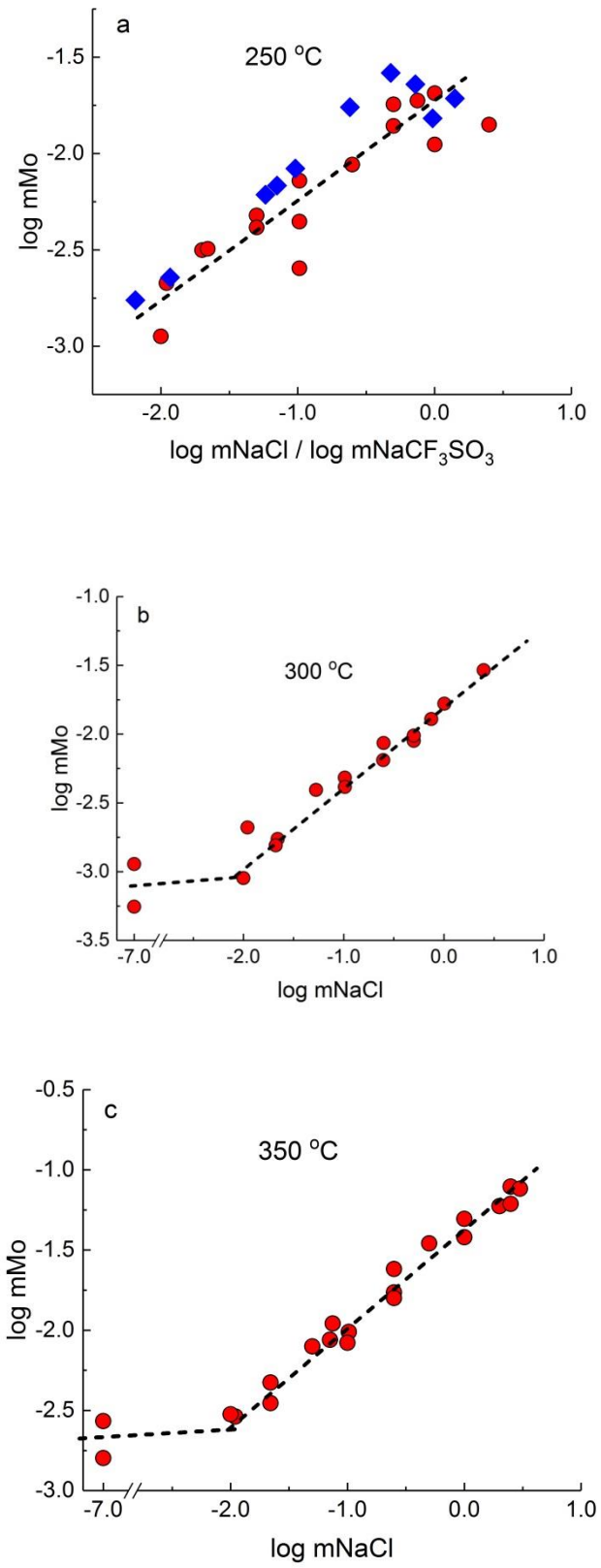

Fig. 2. The logarithm of Mo molality as a function of the logarithm of NaCl molality at 250, 300

and 350 °C (red dots) and as a function of the logarithm of $NaCF_3SO_3$ (sodium triflate) molality at 250 °C (blue diamonds). The uncertainty for each datum is less than the diameter of the symbol.

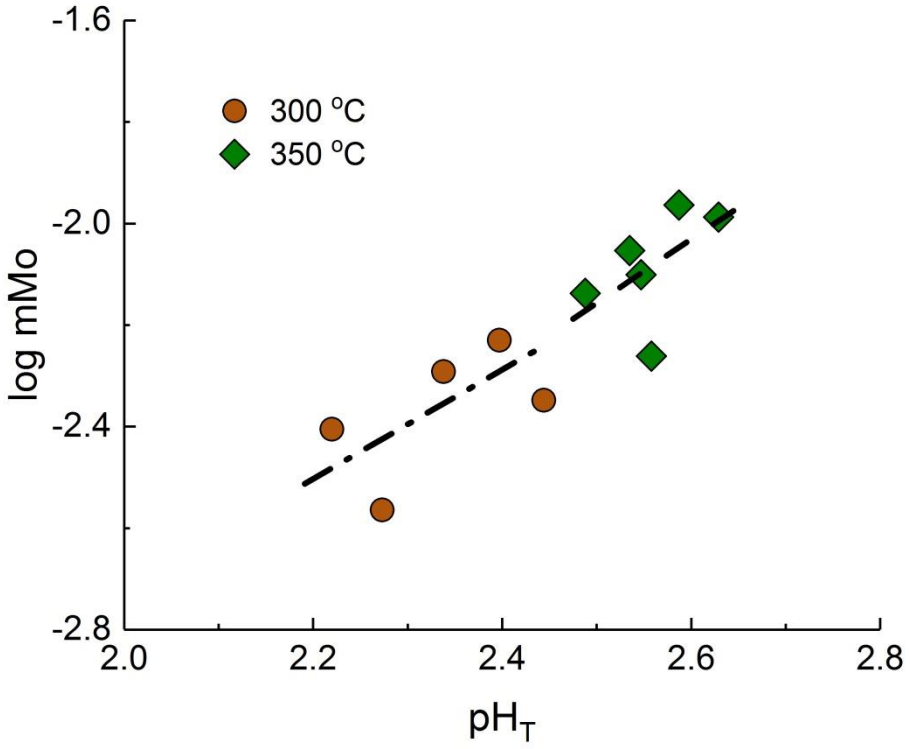

Fig. 3. The logarithm of Mo molality as a function of pH_T at 300 (brown) and 350 (green) °C .

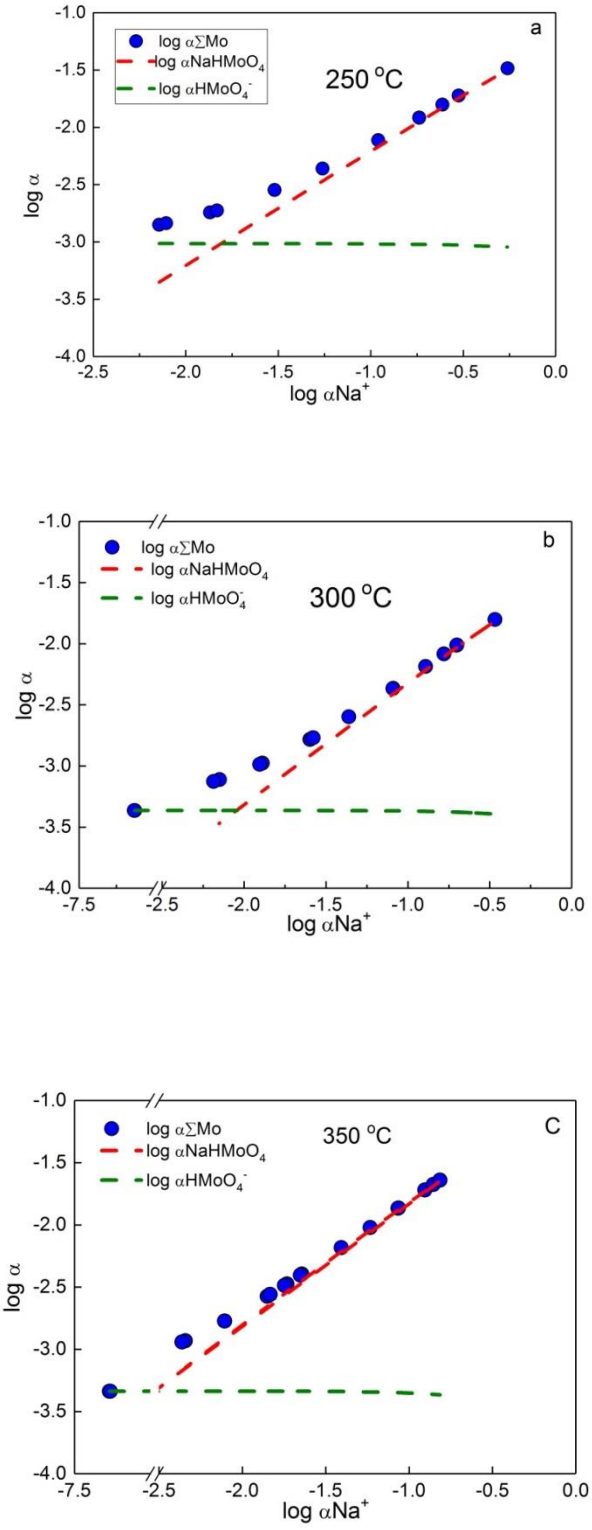

Fig. 4. Values of log a$\sum$Mo (blue dots), log aNaHMoO$_4$ (red dashed line) and log aHMoO$_4^-$ (green dashed line) as a function of log aNa$^+$ at 250 (a), 300 (b) and 350 °C (c). The values were obtained from equilibrium constants for Reactions (1) and (2) calculated using OptimA, and are normalised to a pH of 2.1.

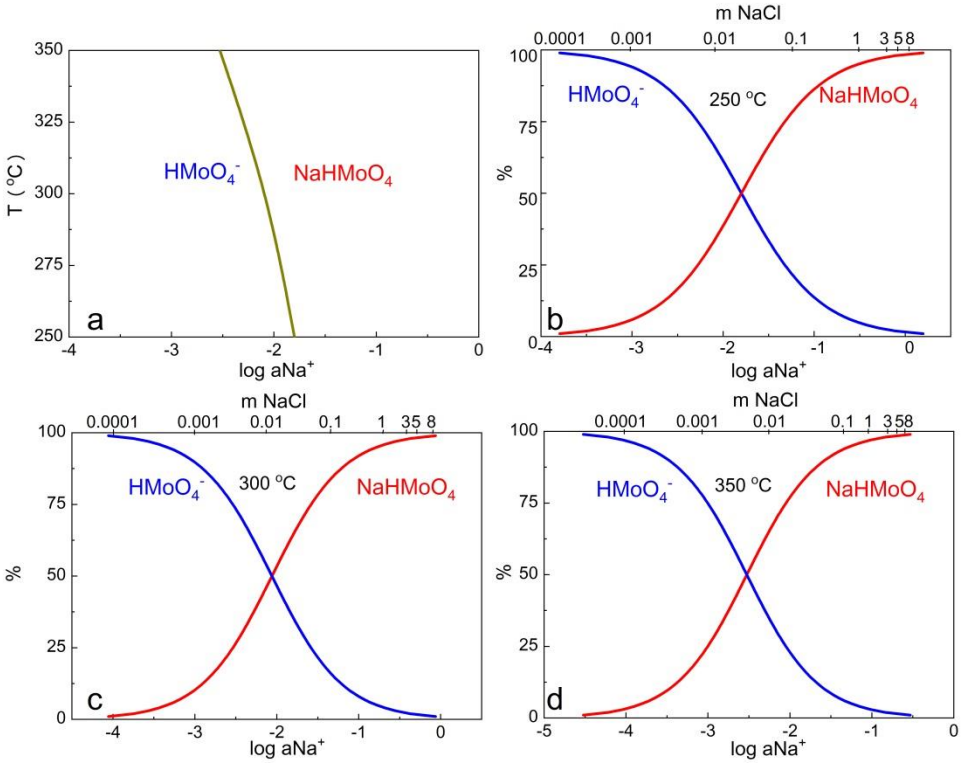

Fig. 5. a) Predominance fields of $HMoO_4^-$ and $NaHMoO_4$ as a function of temperature and log aNa^+. b – d) The distribution of Mo (VI) aqueous species as a function of log aNa^+ at 250 °C, 300°C and 350°C, respectively. The diagrams are based on data for the equilibrium constants of Reaction 3.

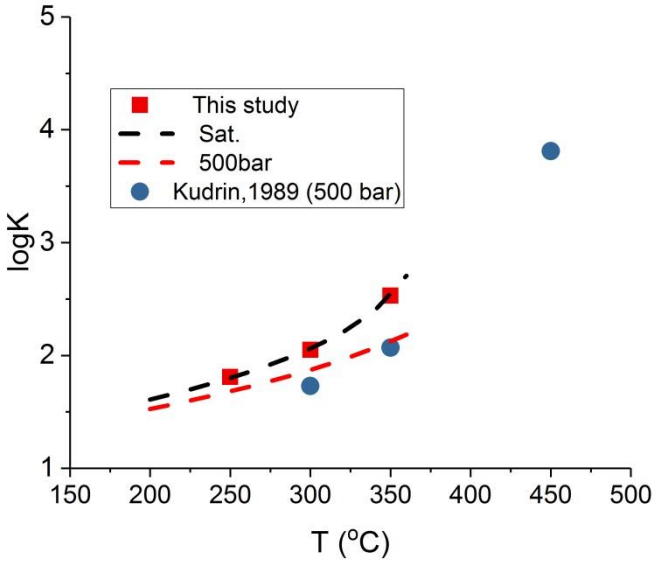

Fig. 6. Equilibrium constants for Reaction 3 determined in this study (red squares), fitted to the BR model (black dashed line) at Psat, and corrected to 500bar (red dashed line) for comparison to the constants derived from Kudrin (1989) for this pressure (blue dots).

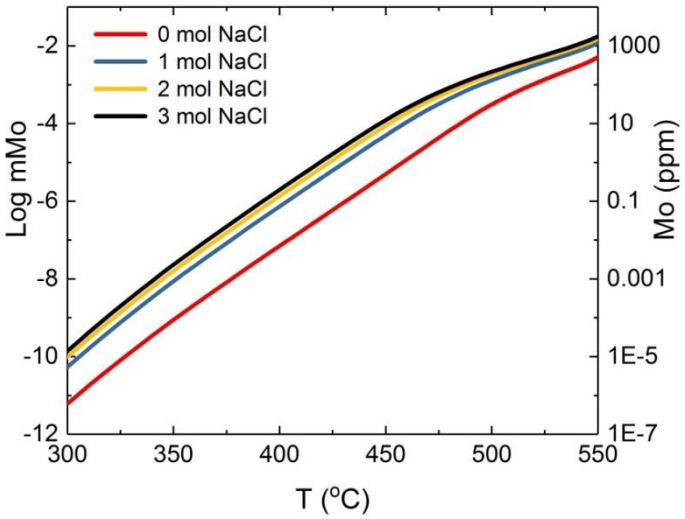

Fig. 7. The concentration of Mo at molybdenite saturation and 1000 bar, as a function of temperature in solutions containing 0 to 3 m NaCl, 0.5 m KCl, and 0.003 m ΣS; pH is buffered by the assemblage, muscovite-K-feldspar-quartz, and fO_2 is fixed at 2.2 log units above the fayalite-magnetite-quartz (FMQ + 2.2) buffer. The calculations were performed using HCh (Shvarov, 2008) and thermodynamic data for aqueous Mo species from this study ($HMoO_4^-$ and $NaHMoO_4$) and Shock, 1997 (H_2MoO_4 and MoO_4^{2-}).

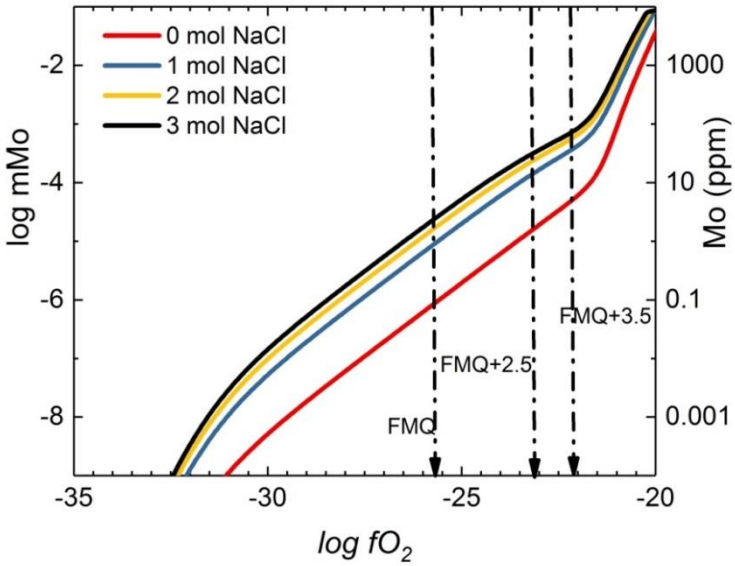

Fig. 8. The concentration of Mo at molybdenite saturation, 450 °C and 1000 bar, as a function of oxygen fugacity in solutions containing 0 to 3 m NaCl, 0.5 m KCl, and 0.003 m ΣS; pH is buffered by the assemblage, muscovite-K-feldspar-quartz. The calculations were performed using HCh

(Shvarov, 2008) and thermodynamic data for aqueous Mo species from this study ($HMoO_4^-$ and $NaHMoO_4$) and Shock, 1997 (H_2MoO_4 and MoO_4^{2-}).